JOURNAL OF MATERIALS SCIENCE 22 (1987) 1908–1912

Magnetic properties of directionally solidified Bi–Mn alloys

M. N. SHETTY, D. K. RAWAT, K. N. RAI
Department of Metallurgical Engineering, Indian Institute of Technology, Kanpur, Uttar Pradesh, India

Microstructure, composition and magnetic property correlations have been attempted for directionally solidified dilute Bi–Mn alloys. The ingots exhibited predominantly acicular BiMn precipitate particles in a bismuth matrix, and showed magnetic anisotropy along the direction of solidification. The saturation magnetization has been found to increase linearly with the weight percentage of manganese over the entire composition range investigated, starting from the hypoeutectic (0.15% Mn) to the hypereutectic (6.6% Mn) region. The intrinsic coercivity has been observed to be a maximum along the direction of solidification, but it decreased with manganese content in both the as-cast and the directionally solidified alloys. The results are discussed in terms of the crystal anisotropy, shape anisotropy and packing factor of the magnetic particles.

1. Introduction

Antiferromagnetic to ferromagnetic transformation in manganese as a result of increasing atomic separation due to alloying with bismuth is of fundamental importance in understanding ferromagnetism in terms of exchange interactions [1]. The magnetic phase BiMn is highly anisotropic and is proposed to be an important permanent magnetic material for a variety of potential applications [2, 3]. The Bi–Mn alloy is also a unique system for investigating the effect of solidification-induced microstructural changes on physical properties [4–6]. This system has a eutectic at 0.5 wt % Mn [7] and the intermetallic BiMn is formed congruently through a peritectic reaction, by recombination of liquid bismuth and solid manganese at a composition of 21 wt % Mn. BiMn is normally prepared by using a slight excess of bismuth for permanent magnet applications [8].

In composite permanent magnets the shape, size, orientation and separation of magnetic particles are important parameters which define the quality of the material. Consideration of these factors has led us to investigate this system for a range of compositions from 0.15 to 6.6 wt % Mn. In this range, isolated BiMn particles are expected to precipitate during solidification of liquids of various compositions. Their shape, size, orientation and packing factor will also change with changing manganese concentration and the method of freezing. The excess bismuth provides a good dispersion medium for BiMn magnetic particles. Also, the ferromagnetic phase BiMn possesses a high degree of compositional stability, and as a result its Curie temperature is fairly constant at 347.5 ± 7.5° C. The magnetic properties such as coercivity and saturation magnetization of the composite Bi–BiMn may then be expected to vary systematically with (i) size, (ii) shape, (iii) orientation, and (iv) packing factor of BiMn particles in addition to an intrinsic dependence on crystalline anisotropy. The present work therefore investigates the effect of composition and mode of freezing on the magnetic properties of Bi–BiMn composites.

2. Experimental procedure

A master alloy was first prepared using high purity bismuth and manganese by induction melting in a vacuum. Further, alloys of desired composition were prepared by adding the required amount of bismuth to the master alloy and melting the charge in an evacuated quartz tube inside a resistance furnace maintained at 700° C. The finally frozen ingots varied in composition from 0.15 to 6.6 wt % Mn. One half of each ingot was used for direct examination of microstructure and magnetic behaviour, and the remaining half was directionally solidified before further investigation.

The directional solidification of the alloy was carried out in a separate vacuum-sealed quartz ampoule held inside a wire cage which was attached to a sufficiently long resistance wire for lowering through a resistance furnace with a fixed temperature profile. Successful directional solidification was achieved by attaching a copper chill rod to the narrow lower end of the quartz ampoule to facilitate unidirectional heat extraction. The resistance wire holding the assembly was connected to a thin flexible copper wire wound over a pulley at the top end of the furnace. This was passed through a wire guide to allow undisturbed lowering through a gear and pulley mechanism attached to a synchronous motor rotating at 1 r.p.m. and with a lowering speed of 3.8 cm h^{-1}. Before the start of solidification, the assembly was first lowered and maintained at 600° C to allow equilibriation of the alloy. The furnace atmosphere was made inert by passing high purity argon to avoid oxidation of the copper chill rod.

0022–2461/87 $03.00 + .12

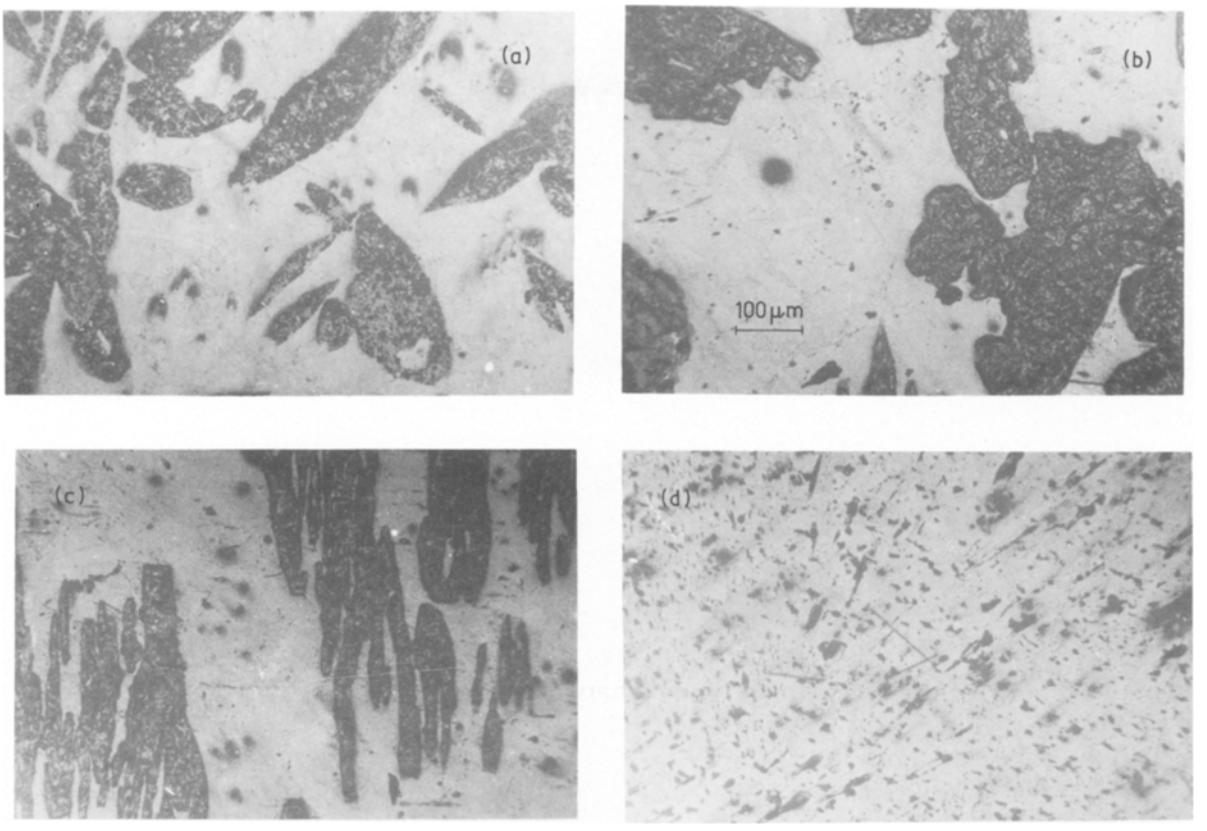

Figure 1 Microstructure: (a) as-cast, 6.6 wt % Mn; (b) directionally solidified, transverse section, 6.6 wt % Mn; (c) directionally solidified, longitudinal section, 6.6 wt % Mn; (d) directionally solidified, transverse section, 0.5 wt % Mn.

Samples from as-cast and directionally solidified ingots were cut to a size of 1 mm × 1 mm × 3 mm and their magnetization characteristics studied using a vibrating sample magnetometer (Princeton Applied Research Corporation, Model 150A) and a Varian electromagnet. The anisotropy in magnetization was studied by applying a fixed magnetic field both along and transverse to the direction of solidification. Pure nickel was used as the standard. Magnetization studies were carried out at room temperature with magnetizing fields upto 10 kOe. The magnetic properties investigated were (i) saturation magnetization, and (ii) coercivity.

For metallographic observations, specimens were sectioned along directions parallel and transverse to the direction of solidification, polished and etched using 2% nitol.

3. Results and discussion

The microstructures of some of these alloys are shown in Fig. 1. In the case of the as-cast hypereutectic alloy (Fig. 1a), predominantly platelet-type particles of magnetic BiMn phase are visible with random orientation. Particles in these composites are generally bigger in size. The microstructures of directionally solidified samples sectioned along and transverse to the direction of solidification are shown in Figs 1b, c and d. It is evident that the second-phase particles are oriented with their longer side along the direction of solidification. In the eutectic composition (0.5% Mn), the acicular particles are smaller and well separated from each other, while those in hypereutectic compositions are much bigger in size (~10 times) and have a tendency to cluster together.

The variation of saturation magnetization (M_s) with composition (wt % Mn) is shown in Fig. 2 for various samples. Except for minor deviations, it increases linearly with the percentage of manganese, because the volume fraction of BiMn is nearly proportional to manganese percentage in the given range. Therefore the saturation magnetization will be proportional to the volume fraction of BiMn phase in these alloys. There is no electronic interaction between excess bismuth and magnetic BiMn. BiMn has a hexagonal structure (a = 0.426 nm, c = 0.608 nm) of the NiAs type [9] with bismuth atoms occupying close-

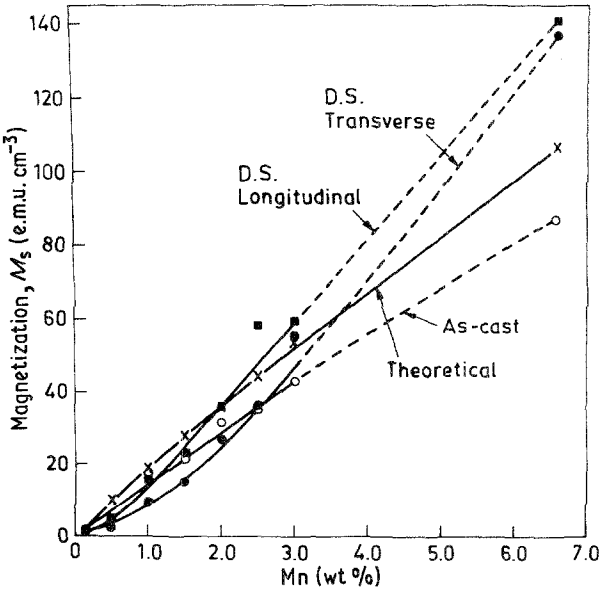

Figure 2 Variation of saturation magnetization with added manganese.

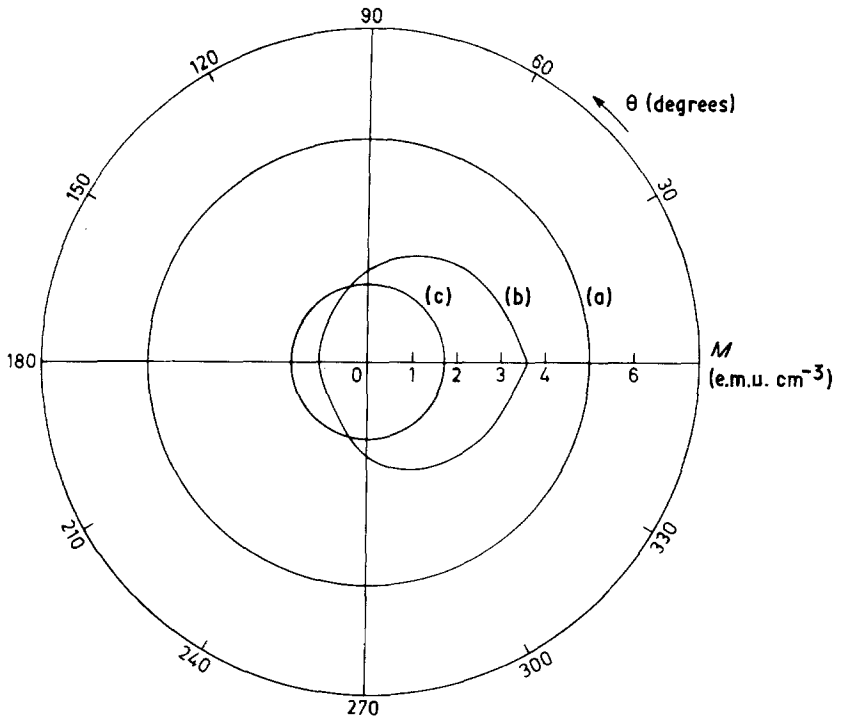

Figure 3 Variation of volume magnetization of Bi–0.5 wt % Mn alloy with rotation of sample in a constant field: (a) as-cast; (b) directionally solidified, field longitudinal; (c) directionally solidified, field transverse.

packed hexagonal positions and manganese distributed at the octahedral sites. The cell contains two molecules of this compound. The atomic magnetic moment of manganese is about $4\,\mu_B$ [7] leading to a saturation magnetization of about 253.86 e.m.u. cm^{-3}. The saturation magnetization values calculated for composites on the basis of various BiMn volume fractions agree well with those measured experimentally.

Magnetization (at fixed field) as a function of sample rotation of as-cast and directionally solidified 0.5% Mn alloys is shown in Fig. 3. Fig. 3a is for the as-cast sample and Fig. 3c is for the directionally solidified sample with the field perpendicular to the solidification direction. The completely isotropic behaviour in both cases may be attributed to a cancellation of particle shape anisotropy arising as a result of the random orientation of particles in all directions in the as-cast samples, and with respect to the transverse direction in the directionally solidified samples. Magnetization of the directionally solidified material with the magnetic field applied along the solidification direction (Fig. 3b) shows anisotropic behaviour as a result of shape anisotropy of the magnetic phase particles. It should be noted that in these cases the microstructure does exhibit BiMn particles preferentially aligned along the direction of solidification.

The variation of coercivity with composition for as-cast and directionally solidified samples is shown in Fig. 4. It passes through a maximum. The coercivity is highest for directionally solidified samples with the field acting along the solidification direction and it is smallest for the as-cast samples. This may be attributed to particle anisotropy, with the easy direction of magnetization likely to lie along the longer axis of the acicular particles, mostly aligned parallel to the direction of solidification. However, it is difficult to isolate the contributions to coercivity from the shape and magnetic crystalline anisotropies because all particles do not possess identical shapes of regular geometry, and information regarding the accurate orientation of particle axis and that of the easy axis of magnetization is lacking. The coercivity due to magnetocrystalline anisotropy $(H_{ci})_{cry}$ and shape anisotropy $(H_{ci})_{sh}$ are expressed in terms of the saturation magnetization M_s

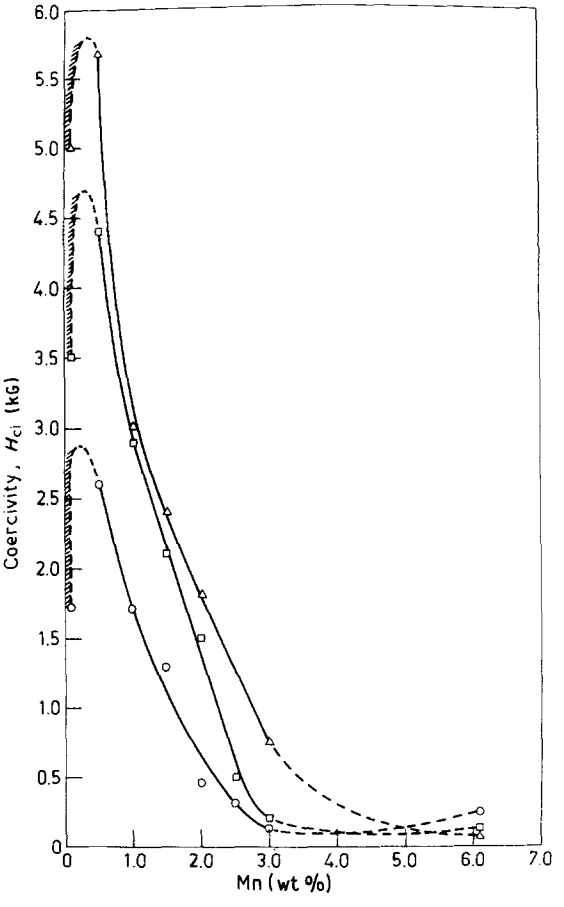

Figure 4 Variation of intrinsic coercivity H_{ci}, with added manganese. Measurements at the lower concentration limits (hatched) are somewhat uncertain. (○) As-cast; (□) directionally solidified, transverse section; (△) directionally solidified, longitudinal section.

(e.m.u.) as given below [10]:

$$(H_{ci})_{cry} = 2K/M_s \quad (1)$$

$$(H_{ci})_{sh} = (N_a - N_c)M_s \quad (2)$$

where K is the magnetocrystalline anisotropy constant and N_c and N_a are, respectively, the demagnetization factors along the longitudinal and transverse axes of rod-shaped particles. Generally, for long and slender particles $N_c \simeq 0$ and $N_a \simeq 2\pi$. In the present work, the average ratio of length to diameter is found to be about 10. Therefore, taking $N_a - N_c \simeq 6$ and substituting the usual values of $M_s = 254\,\text{erg Oe}^{-1}\,\text{cm}^{-3}$, $K = 9 \times 10^6\,\text{erg cm}^{-3}$ (1 erg $= 10^{-7}$ J), one finds that $(H_{ci})_{cry} \simeq 70$ kOe and $(H_{ci})_{sh} \simeq 1.5$ kOe. Thus the coercivity may be expected to be about 70 ± 1.5 kOe, the plus and the minus sign being taken depending upon whether the crystalline and the shape anisotropies complement each other or not. Our maximum observed coercivity of about 5 kOe is considerably lower than this expected value and we examine below some of the causative factors.

It is implicit in Equation 1 that magnetic reversal can be brought about by coherent spin rotation in single domain particles which require high fields. The same could also be achieved by domain nucleation and its growth by domain wall motion at much smaller fields. In addition, the idea of incoherent rotation involving fanning and curling has also been proposed by earlier workers as leading to significant lowering in the coercive field [11–13]. Magnetic reversal by domain nucleation and consequent movement of domain walls in a single domain particle becomes easier if some structural defects like dislocations, bumps and sharp corners exist [14]. At these structural defects the presence of intense magnetostatic fields necessitate the formation of closure domains leading to the formation of domains of reversed spins. Hence, no additional energy is required for the nucleation of fresh domains in the reversed orientations. What is now needed is to unpin the domain walls from the defect sites at an insignificant expense of energy, thus leading to a greatly reduced coercive force. This has found firm support in the experimental work of DeBlois and Bean [15]. For instance, the intrinsic coercivity of single-domain iron is 560 Oe. However, these workers found that the amount of reversing field could vary from about 500 to 25 Oe in iron whiskers of 12.5 μm diameter. The field corresponding to the imperfect region of the whiskers was invariably the lowest. In the present case, the average particle size of BiMn of about 40 μm is much larger than that required for a single domain. For cubic or spherical shapes, the single critical domain size L_c of BiMn can be readily calculated from the expression [10]

$$L_c = 1.7\gamma/\pi^2 M_s^2 \quad (3)$$

where γ is the domain wall energy. If we take $\gamma \simeq 10\,\text{mJ m}^{-2}$, we get L_c to be about 0.25 μm. If we assume rod-like particles the critical size will become larger by an order of magnitude [16, 17]. However, our average particle size is quite large, leading to the existence of a multi-domain structure within individual particles. This could considerably lower the coercivity values.

Some of the other factors that contribute to the observed variation in coercivity, which passes through a maximum with manganese concentration, are particle size and interparticle separation. At very low manganese contents, magnetization is not stable because of the near absence of the magnetic phase. With increasing manganese concentration the particle size increases, but the particle-to-particle distance decreases. A variation of coercivity with particle size, somewhat similar to that of the present investigations, has been found by Luborsky [18] for ferromagnetic and ferrimagnetic particles. It has also been found to change according to the relation [19]

$$H_{ci} = A - \frac{B}{L^{3/2}} \qquad L \leqslant L_c \quad (4)$$

$$H_{ci} = a + \frac{b}{L} \qquad L \geqslant L_c \quad (5)$$

where A, a, B, b are temperature-dependent constants and L as before is the particle size. The coercivity has a maximum just at the single domain size L_c. The dependence for $L < L_c$ is well understood in terms of a superparamagnetic interaction between small magnetic particles. The cause of variation for $L > L_c$ is not yet well understood.

In a composite material a measure of the interparticle separation of a particular phase may also be represented by its volume fraction or packing fraction, p. An empirical expression involving packing fraction and intrinsic coercivity for a particle having shape anisotropy is of the form $H_{ci} = H_{ci}(0)\,(1 - p)$, where $H_{ci}(0)$ is the intrinsic coercivity of an isolated particle [10, 20]. This relationship is particularly valid at higher concentrations in Fig. 4, where the particles are bigger and show a tendency to cluster together. At lower concentrations the particles are smaller, have a uniform distribution, and remain well separated from each other. Fig. 5 shows the hysteresis loops for the eutectic alloy where the particle size and distribution are quite uniform. The increased anisotropy in the directionally solidified samples in comparison with the as-cast samples is also reflected in a much bigger hysteresis loop. Therefore, in view of the foregoing discussion, we may initially expect the coercivity to increase at low concentrations until an optimal particle size of the magnetic phase is reached and, a decrease with further increase in the manganese concentration. In this way it is possible to combine crystal and shape anisotropies along with the packing fraction of magnetic particles to explain the observed dependencies.

4. Summary

Dilute, magnetically anisotropic Bi–Mn alloys have been produced by directional solidification. The alloys contain magnetic BiMn particles preferentially aligned along the direction of solidification. The magnetic properties of the as-cast and directionally solidified alloys have been compared and the observations related to the anisotropy, size and separation of BiMn particles in the bismuth matrix.

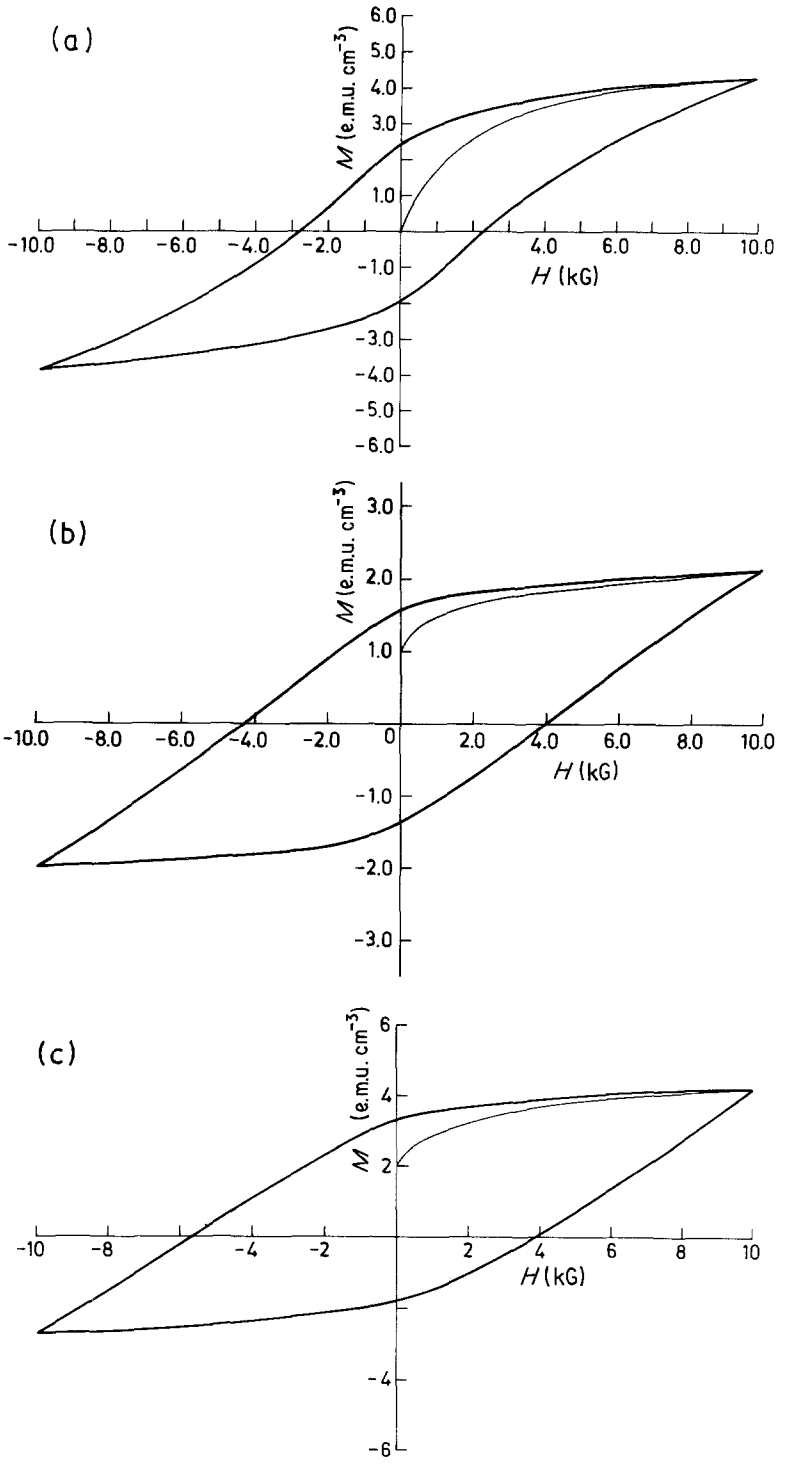

Figure 5 Hysteresis loops for Bi–0.5 wt % Mn: (a) as-cast; (b) directionally solidified, transverse section; (c) directionally solidified, longitudinal section.

References

1. J. C. SLATER, *Phys. Rev.* **36** (1930) 57.
2. J. J. BECKER, *IEEE Trans. Magn.* **4** (1968) 239.
3. A. GORE, K. TOLSUJI and O. TSUTOMU, US Patent 4 482 578 (1984); Japanese Patent (Appl.) 8 211 004 (1984).
4. F. R. MOLLARD and M. C. FLEMINGS, *Trans. TMS-AIME* **293** (1963) 1534.
5. M. TASSA and J. D. HUNT, *J. Cryst. Growth* **34** (1976) 38.
6. J. L. DeCARLO and R. G. PIRICH, *Metal Trans.* **15** (1984) 2155.
7. A. U. SEYBOLT, H. HANSEN, B. W. ROBERTS and P. VURCISIN, *J. Metals* **8** (1956) 607.
8. R. J. PARKER and R. J. STUDDERS, "Permanent Magnets and Their Applications" (Wiley, New York, 1962) p. 83.
9. P. M. HANSEN, "Constitution of Binary Alloys" (McGraw-Hill, New York, 1958) p. 321.
10. B. D. CULLITY, "Introduction to Magnetic Materials" (Addison-Wesley, London, 1972) pp. 338, 310 and 387.
11. I. S. JACOBS and C. P. BEAN, *Phys. Rev.* **100** (1955) 1060.
12. F. B. WILLIAM Jr, "Magnetostatic Principle in Magnetization" (North-Holland, Amsterdam, 1962) p. 202.
13. E. H. FREI, S. SHTRIKMAN and D. TREVES, *Phys. Rev.* **106** (1957) 446.
14. C. KITTEL and J. K. GALT, *Solid State Phys.* **3** (1956) 437.
15. R. W. DeBLOIS and C. P. BEAN, *J. Appl. Phys.* **30** (1959) 225S.
16. E. C. STONER and E. P. WOHLFARTH, *Phil. Trans. R. Soc.* **A240** (1948) 599.
17. P. J. GRUNDY and R. S. TEBBLE, *Adv. Phys.* **17** (1968) 153.
18. F. E. LUBORSKY, *J. Appl. Phys.* **32** (1961) 171S.
19. C. P. BEAN and J. D. LIVINGSTON, *ibid.* **30** (1959) 120S.
20. G. T. RADO and H. SUHL (eds), "Magnetism" Vol. III (Academic, New York, 1963) p. 351.

Received 24 March
and accepted 11 November 1986